



Prediction of the pollutants movements from the polluted industrial zone in 10th of Ramadan city to the Quaternary aquifer

Enas E. Hussein¹ · Moharram Fouad² · Mohamed I. Gad³

Received: 11 June 2018 / Accepted: 9 January 2019 / Published online: 21 January 2019
© The Author(s) 2019

Abstract

There are some sources of pollution of the groundwater such as the industrial, agriculture, domestic activities and the oxidation ponds that are considered collection points for waste disposal plants. The motivations to do this work were: (1) investigating the concentrations of pollutants in the oxidation ponds and well surrounding the 10th Ramadan city and (2) predicting the groundwater flow and the pollutant transport to the groundwater from the pollution source using a numerical simulation (MODFLOW-2000 with MT3D code). The samples of groundwater were collected from the wells that spread around the studied area as well as many samples were collected from the oxidation ponds to investigate the concentrations of pollutants in these samples and predict the pollutant transport to the groundwater over 30 years. The results illustrated that the ion concentration of most samples from the oxidation ponds resources contained Al^{3+} , Fe^{2+} , Sr^{2+} , Ni^{2+} , and Cr^{2+} which were exceeding the acceptable limit of WHO (International standards for drinking water, WHO, Geneva, 1996) standards. The results also demonstrated that most of the analyzed groundwater samples are polluted with strontium (Sr^{2+}), aluminum (Al^{3+}), and iron (Fe^{2+}). The simulation predicted that the pollutants movements toward the northeast of the study zone over a long-term period (30 years).

Keywords Groundwater · Pollution · Pollutants · MODFLOW · Agricultural · Domestic · Industrial activities · Heavy metals · Oxidation ponds · 10th of Ramadan city

Introduction

Egypt faces water scarcity conditions, and freshwater availability is insufficient to cover annual needs. It aims to use its limited water resources efficiently and bridge the gap between supply and demand. In addition, the Egyptian water policy aims to augment the quantity of available water and maintain the surface and groundwater quality. Therefore, groundwater resources play an important role in saving freshwater, and it is considered a lifeline of new communities and remote areas. The pollution of the groundwater led to the shortfall in the water that was suitable for drinking

purpose (Tirkey et al. 2017). Groundwater becomes polluted when people-created substances are dissolved or mixed in waters, and these substances were recharged to the aquifer via its movement (Nariman et al. 2011). There are different sources of groundwater pollution, such as road salt, petroleum products leaking from underground storage tanks, nitrates from the overuse of chemical fertilizers or manure on farmland, excessive applications of chemical pesticides, acid rain, and septic tanks, domestic activities, leaching of fluids from landfills and dumpsites, and accidental spills [US Environmental Protection Agency (EPA)]. On the other hand, the most important sources of groundwater pollution in the 10th of Ramadan city are industrial, agricultural, domestic activities, and oxidation ponds which all could affect groundwater quality depending on several factors including, but not limited to, the type of soil, the amount and type of the pollutants and the land topography (Wu and Sun 2016). Industrial activity is one the most dangerous source of pollution of the groundwater and varies depending on the type of industry, the way of disposing of the output, and the contents of the heavy elements (Chintalapudi et al. 2017).

✉ Enas E. Hussein
Ali.enas75@yahoo.com

¹ National Center of Water Research, Cairo, Egypt

² Engineering Department of Public Works, Faculty of Engineering, Mansoura University, Mansoura, Egypt

³ Hydrology Department, Desert Research Center, Cairo, Egypt

Rainfalls and waste dissolution resulted in infiltration of the associated heavy metals from domestic, industrial, or agricultural activities to the groundwater (Waseem et al. 2014), which are recognized as severe pollutants, and have adverse implication in a short time and/or long time on humans and ecosystems.

The studies that have been done to measure the concentrations of the pollutants through collecting samples from wells surrounding the study area or through samples taken from oxidation ponds were reviewed, and in addition, the studies that have been concerned with the use of numerical mathematical methods and modern software codes in tracking these pollutants and how they reach groundwater (Banejad et al. 2014) were also reviewed as follows:

Since 1980s, oxidation ponds collect the effluents of domestic wastewater from the urban and part of heavy industrial wastewater. These ponds were used to drain the industrial effluents and domestic wastewater into wadi El-Watan, which located 15 km northeast of the 10th of Ramadan city using natural and artificial canals to threat El-Shabab freshwater canal. The total surface area of these three oxidation ponds was 1.3 million m² since 1997 and reaches now to more than 5 million m² (Taha et al. 2004), and it is concluded that the Quaternary aquifer was polluted with nitrates and phosphates (NO₃⁻, PO₄⁻), while the groundwater of Miocene and Oligocene aquifer was not polluted by trace and minor elements.

The oxidation ponds, especially oxidation pond no. III (industrial effluents), were polluted by higher concentrations of Fe⁺⁺ and Mn⁺⁺, and the soil covers of the new reclaimed land around the oxidation ponds, which irrigated with wastewater, were polluted by heavy metals Cu⁺⁺, Fe⁺⁺, Mn⁺⁺, and Zn⁺⁺. The infiltration of polluted wastewater to groundwater is obvious, especially close to the oxidation ponds (Embaby and El Haddad 2007). Heavy metals (Cu, Fe, Mn, and Zn) were accumulated in soil and plants irrigated with the wastewater of 10th of Ramadan city (Embaby 2009). The efficacy of the oxidation ponds on the outskirts of the 10th of Ramadan city in mineralizing some industrial pollutants was low (Tawfic et al. 1999). The oxidation ponds in the study area have high concentrations of heavy metals, NO₃, PO₄, TDS, TSS, BOD, and COD than Egyptian law 93/62 and are not constructed to be an environmentally safe especially on the groundwater (Abu El Ela 2008).

El Sayed et al. (2012) studied the groundwater pollution from oxidation ponds in the 10th of Ramadan city. They concluded that all samples of surface water exceed detection limit of Al³⁺ ion concentration. All samples of oxidation ponds are polluted by Al³⁺, Fe³⁺, B³⁺, Mo²⁺, and PO₄. Some samples of groundwater have concentration of Fe³⁺, Al³⁺, Mo²⁺, and B³⁺ higher than the permissible limit. Most of the samples have a high pollution level of BOD and COD

than the acceptable level of pollution. Some of the collected samples contain bacterial pollution.

Most of researches that were focused on the pollutant migration of groundwater due to different activities such as industrial, agriculture, and domestic utilized one of the common software code MODFLOW and MODPTHA (El Araby and El Arabi 2008; Mondal 2005; Saghravani and Mustapha 2011; Banejad et al. 2014; Ayvaz 2016; Datta et al. 2017). The model was calibrated in steady-state condition, and the results of calibration showed that the error between observed head and computed head is in allowable range also, the computed water level flow follows the general slope of the area. Furthermore, MODPATH code was used for estimation of flow path-lines and travel time of pollutants. Finally, MODFLOW and MT3D are the most commonly used simulators for groundwater flow and solute transport in subsurface systems, respectively (Abu-El-Sha'r and Hatamleh 2007).

In this paper, the concentration of the heavy metals in the oxidation ponds was investigated. The chemical analysis was performed with many samples that were collected from several wells in the surrounding area as well as the oxidation ponds to study the pollution levels of the groundwater with the heavy metals. In addition, software MODFLOW-MT3D based on the numerical solution of the flow equation was used to follow the path of these heavy metals to the groundwater. Prediction of the pollutant transport was also investigated over 30 years from the instant of collecting the samples.

Location, climatic, topographical, and hydrogeological features of the study area

Location

The 10th of Ramadan city is one of the early and large industrial settlements that emerged in the last four decades. It is located in Cairo-Ismailia desert road at 55 km far from Cairo. It lies between latitude 30°17' and 30°25'N and longitude 31°34' and 31°49'E with an area of about 465 km². It is bounded by El Shabab canal from east, El Asher-Belbes road from the west, Ismailia Canal from north and Cairo-Ismailia desert roads from the south (Fig. 1).

Climate

The study area is characterized by the desert climate with arid. The winter months represent the rainy season with a scarce amount of precipitation, while the summer months

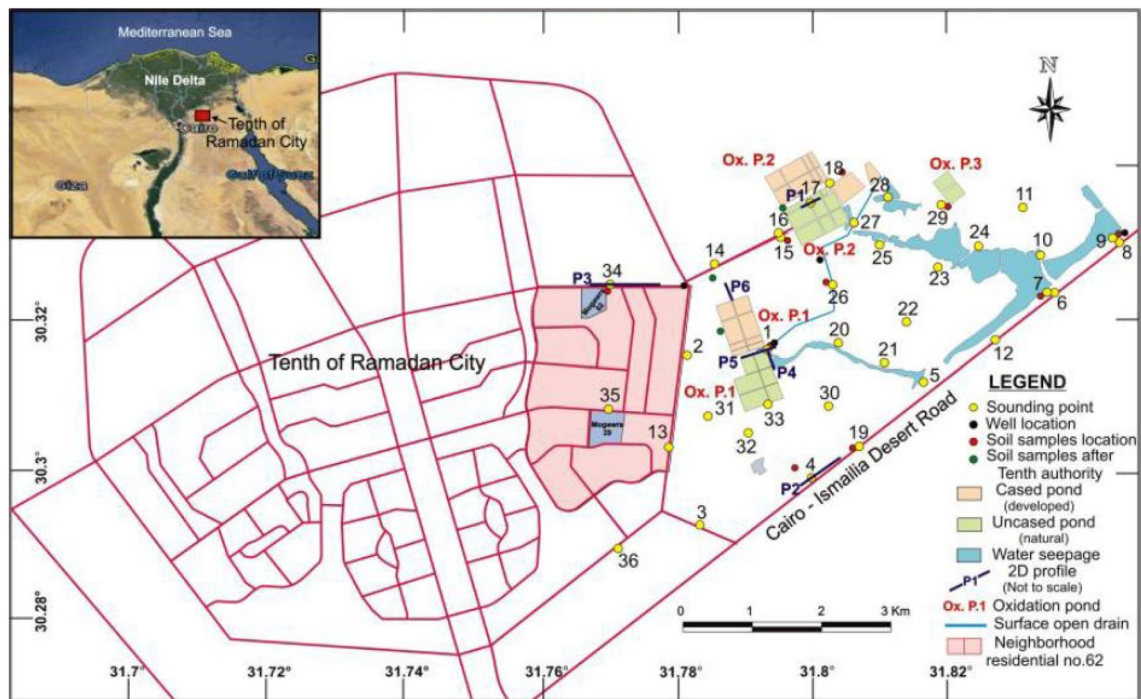


Fig. 1 Location map of 10th of Ramadan city, including the oxidation ponds 1, 2 and 3. (Attwa et al. 2013)

are dry. Evaporation is very high and increases from north to south. The amount of recharge of groundwater aquifers and the groundwater quality is influenced by both precipitation and evaporation.

Topography

The 10th of Ramadan city shows variable topographic features where the ground elevation rises from 12 m above mean sea level in the north, to about 80 m in the south. The studied area shows a general slope towards the northern and northeastern direction.

It is important to note that the 10th of Ramadan city rests on the Pleistocene permeable sandstone formation that represents the hosting formation of the most groundwater aquifer in the Nile Delta, where the groundwater represents the main source of fresh water in the study area. In the last few years, agricultural, agro-industrial, and sustainable development projects were expanded rapidly around the surface and groundwater resources, and therefore, the wastewater drainage causes a great danger to the groundwater aquifer if they are not designed to keep their pollutants away from the surrounding soil and water systems. Therefore, protecting groundwater from pollution is very important. Hence, hydrological and hydrochemical studies are the base road for simulation of groundwater pollution.

Hydrogeology

The aquifer in the study area is considered as free aquifer relating to the Quaternary aquifer of the Nile Delta, which represents the main aquifer especially in the northern part of the study area. It consists of graded sand and gravel intercalated with clay lenses and overlain by silt and clay layers. The total saturated thickness of the Quaternary aquifer increases gradually from south to north with the change from a few meters in the southern parts to more than 240 m in the northern parts of the study area (Gad 1995). The Quaternary aquifer is mainly recharged by seepage from Ismailia Canal and the other subsidiary irrigation canals, in addition to the infiltration from the new reclaimed sandy soils (El-Haddad 2002), while the Miocene aquifer occupies the southern part of the study area. It is overlain by about 200 m of Quaternary deposits. The Quaternary aquifer may be contaminated with different sources which may present in the unsaturated zone. The hydraulic conductivity K (m/day), transmissivity T (m^2/day), and storage coefficient S (m^{-1}) (or specific yields for unconfined aquifers) are the main hydraulic parameters for determining water flow, water table response, and groundwater resources pollutant. They govern the inflow and outflow routes of the groundwater systems. The flow of water and hydraulic properties through the vadose zone play a great role, especially in the study of aquifer pollution since this zone is the link between surface water and

groundwater. It controls the recharge, discharge, and pollutants movement routes in the saturated zone. The pumping test is one of the best ways in evaluating hydraulic parameters of aquifers. Summary of the previous pumping tests were recorded in the 10th of Ramadan city (Gad 1995, Table 1).

The main objects of the hydrological study of any area is to construct a water table map, showing the flow direction, areas of recharge, areas of discharge, and hydraulic gradient. Due to the wide reclamation activities and other desert developments in the study area, many of the drilled wells are equipped with water pumps; however, these prevent the measuring of water levels. The water levels are measured only in some wells from the studied area. According to these measurements, water table map 1992 (Gad 1995) (Fig. 2) and water table map 2005 (Gad et al. 2015, Fig. 3) were constructed. This is considered the water table of the groundwater aquifer covering the 10th of Ramadan city.

Hydrochemistry of the wastewater of the oxidation ponds

The study of the hydrochemical aspects of the wastewater oxidation ponds in the study area is mainly based on the results of the chemical analyses of eight selected water samples that were collected from the wastewater oxidation ponds in December 2010 and July 2012, respectively (Table 2). Complete chemical analyses were carried out in the laboratory of the Desert Research Center as well as the archival data from literatures to clarify the main different pollutants from industrial, domestic, and agricultural activities which concentrated in these oxidation ponds.

The results showed that the chemical inorganic concentration of Ba^{2+} , B^{2+} , Co^{2+} , Cd^{2+} , Cu^{2+} , Mn^{2+} , and Zn^{2+} in all wastewater oxidation ponds samples are below the permissible levels of WHO (1996) standard (2.0, 1.0, < 0.05, 0.005, < 0.05, 0.2, and 5.0 mg/l, and these values are the

Table 1 Summary of calculating aquifer parameters in the study area. (After Gad 1995)

Locality	Symbol	Transmissivity (T) m ² /day	Storativity (S) dimensionless	Diffusivity (D) m ² /day
Northern part	N1	19,986	0.0004	49,965,000
Northern part	N2	40,600	0.0001	
Northern part	N3	20,500	0.0001	
Northern part	N4	35,600	0.0011	
Middle part	M1	5947	0.0084	707,976.19
Middle part	M2	17,858	0.0009	19,842,222
Southern part	S1	9381	0.0117	
Southern part	S2	4784	0.0025	1,913,600
Eastern part	E1	752	0.0003	2,506,666.7
Western part	W1	21,600	0.0145	1,489,655.2
Western part	W2	32,100	0.0208	1,543,269.2
Western part	W3	16,000	0.0097	

Fig. 2 Water table contour map of the selected groundwater wells during Dec 1992. (After Gad 1995)

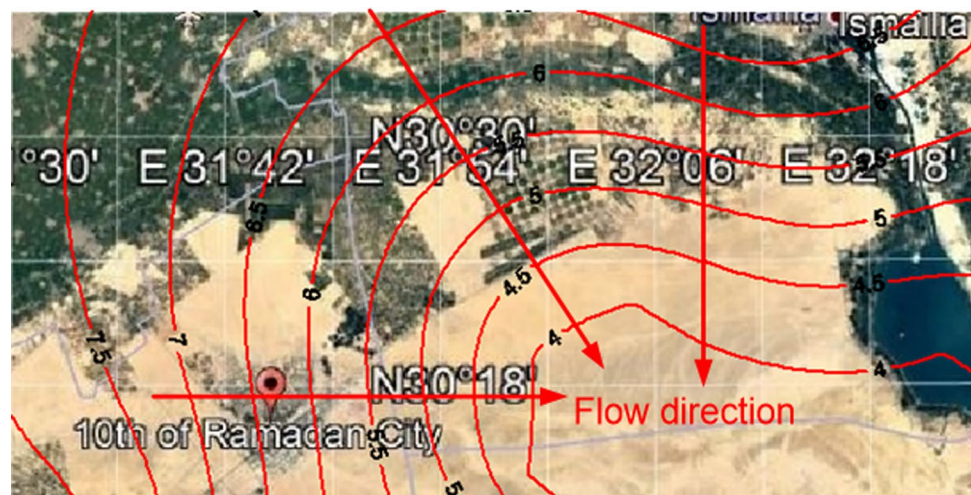


Fig. 3 Water table contour map of the selected groundwater wells during Dec 2005 (After Gad et al. 2015)

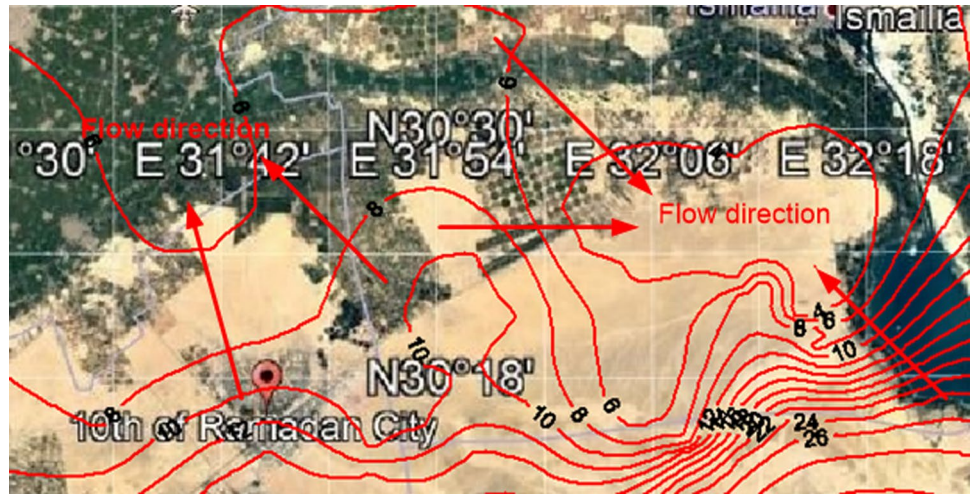


Table 2 Chemical inorganic and biological analysis of wastewater samples in the 10th of Ramadan city expressed in mg/l (2010, 2012)

Pollutant	Recommend max. conc. (mg/l)	Location (2010) in mg/l			Location (July 2012) in mg/l				
		Pond no. 1	Pond no. 2	Pond no. 3	Pond no. 1	Pond no. 2	Pond no. 3	Inflow station	Outflow station
pH	–	6.4	6.4	5.8	6.7	6.8	7.6	8.9	6.8
E.C.	–	1612	1563	3520	1764	2108	2748	4230	1358
TDS	–	1032	1000	2253	1129	1383	1766	2299	922
Al	0.2	0.517	0.219	0.695	0.185	0.118	0.458	0.583	0.487
B	1	0.162	0.269	0.397	0.269	0.277	0.292	0.184	0.157
Ba	2.0	0.079	0.079	–	0.085	0.2545	1.338	–	–
Cd	0.005	0.0007	0.0007	–	0.0009	0.0006	0.0006	–	–
Co	<0.05	0.0031	0.0031	–	0.003	0.0009	0.001	–	–
Cr	0.01	0.074	0.07	0.048	0.034	0.038	0.058	0.043	0.041
Cu	<0.05	0.0241	0.0334	0.007	0.0109	<0.009	<0.009	0.0123	<0.009
Fe	0.3	0.552	0.215	1.670	0.118	0.147	4.357	2.263	1.136
Mn	0.2	0.092	0.095	0.114	0.067	0.109	0.205	0.105	0.065
Mo	0.05	<0.0008	<0.0008	<0.0008	<0.0008	<0.004	<0.004	<0.004	<0.004
Ni	0.01	0.056	0.045	0.032	0.034	0.032	0.047	0.045	0.0389
Pb	0.05	<0.004	<0.004	<0.004	<0.004	<0.006	<0.006	<0.006	<0.006
Sr	0.11	0.528	0.526	0.491	0.588	0.552	0.508	0.535	0.491
V	0.01–0.1	<0.01	<0.01	<0.01	<0.01	<0.01	<0.01	<0.01	<0.01
Zn	5	0.117	0.047	0.122	0.026	0.021	0.141	0.245	0.178
No ₃	45	136.5	80.0	120.0	94.2	159.0	181.3	85.9	43.0
Po ₄	1	16.147	16.184	20.947	13.73	30.04	55.02	104.14	23.3

maximum allowed concentration levels of those chemicals), respectively. Moreover, most samples of wastewater oxidation ponds were polluted with Fe²⁺ and Al³⁺ ions, while all wastewater oxidation ponds samples were polluted with Sr²⁺, Cr²⁺, and Ni²⁺, and this reflect industrial and domestic activities in the study area. The chemical and biological results in most wastewater oxidation pond samples indicated high concentrations of NO₃ and PO₄ than

the permissible level (Table 2) as a result of the excessive usage of agricultural fertilizers.

The spatial and temporal variations of chemical inorganic pollutants (heavy metal pollutants) in oxidation ponds in the 10th of Ramadan city were examined (Tables 3, 4, 5). There was a high level of variability among locations within each oxidation pond to study the spatial variation of the pollutants in July 2012 between the different oxidation

Table 3 Concentration of chemical inorganic pollutants (mg/l) resulted from the analyzed samples of wastewater of pond no. 1

Date of analysis Heavy metal	Concentration of heavy metal in mg/l				
	Oct-2001 ^a	Jul-2006 ^a	Jul-2008 ^a	Dec-2010	Jul-2012
Aluminum (Al)	0.1	0.15	0.2	0.5174	0.185
Boron (B)	0.1	0.15	0.26	0.1623	0.269
Barium (Ba)	0.01	0.03	0.06	0.079	0.085
Cadmium (Cd)	0.0019	0.002	0.0003	0.0007	0.0009
Cobalt (Co)	0.001	0.001	0.002	0.0031	0.003
Chromium (Cr)	0.091	0.07	0.04	0.0735	0.034
Copper (Cu)	0.0091	0.01	0.04	0.0241	0.0109
Iron (Fe)	0.1	0.17	0.17	0.5523	0.118
Manganese (Mn)	0.03	0.06	0.08	0.0921	0.067
Molybdenum (Mo)	0.002	0.003	0.002	0.00078	0.00079
Nickel (Ni)	0.0091	0.02	0.05	0.0561	0.034
Lead (Pb)	0.06	0.07	0.008	0.00394	0.0048
Strontium (Sr)	0.5	0.55	0.65	0.5228	0.588
Vanadium (V)	0.002	0.004	0.007	0.0091	0.009
Zinc (Zn)	0.019	0.04	0.05	0.1174	0.026

^aThese data are compiled from previous works (10th of Ramadan city's Council, Embaby and El-Haddad 2007; DRC 2008)

Table 4 Concentration of chemical inorganic pollutants (mg/l) resulted from the analyzed samples of wastewater of pond no. 2

Date of analysis Heavy metal	Concentration of heavy metal in mg/l				
	Oct-01 ^a	Jul-06 ^a	Jul-08 ^a	Dec-10	Jul-12
Aluminum (Al)	0.1	0.2	0.3	0.2194	0.1182
Boron (B)	0.03	0.07	0.09	0.269	0.2773
Barium (Ba)	0.01	0.02	0.031	0.0469	0.2545
Cadmium (Cd)	0.0002	0.0004	0.0006	0.0007	0.00058
Cobalt (Co)	0.0012	0.0015	0.0018	0.0021	0.0009
Chromium (Cr)	0.01	0.05	0.07	0.0704	0.0381
Copper (Cu)	0.01	0.02	0.03	0.0334	0.009
Iron (Fe)	0.1	0.24	0.2	0.2146	0.1474
Manganese (Mn)	0.1	0.15	0.04	0.0008	0.1089
Molybdenum (Mo)	0.002	0.002	0.0027	0.0447	0.0039
Nickel (Ni)	0.009	0.02	0.03	0.0447	0.0322
Lead (Pb)	0.027	0.029	0.02	0.0038	0.0059
Strontium (Sr)	0.2	0.3	0.39	0.5262	0.552
Vanadium (V)	0.03	0.03	0.04	0.009	0.009
Zinc (Zn)	0.019	0.04	0.3	0.0468	0.0213

^aThese data are compiled from previous works (10th of Ramadan city's Council, Embaby and El-Haddad 2007; DRC 2008)

ponds. It was found that the spatial variation in Zn concentration fluctuated from 0.0213 to 0.1408 mg/l, Mn concentration fluctuated from 0.067 to 0.2054 mg/l and from 0.0048 to 0.006 mg/l for Pb concentration. Moreover, the spatial variation in Al concentration fluctuated from 0.1182 to 0.4582 mg/l, B concentration fluctuated from 0.269 to 0.2916 mg/l, Cr concentrations fluctuated from 0.034 to 0.0578 mg/l, the Fe concentration from 0.118 to 4.357 mg/l,

Table 5 Concentration of chemical inorganic pollutants (mg/l) resulted from the analyzed samples of wastewater of pond no. 3

Date of analysis Heavy metal	Concentration of heavy metal in mg/l				
	Oct-01 ^a	Jul-06 ^a	Jul-08 ^a	Dec-10	Jul-12
Aluminum (Al)	0.1	0.5	0.8	0.6953	0.4582
Boron (B)	0.18	0.2	0.29	0.3972	0.2916
Barium (Ba)	0.01	0.02	0.031	0.0921	1.338
Cadmium (Cd)	0.0002	0.0004	0.0006	0.0007	0.0006
Cobalt (Co)	0.0012	0.0015	0.0018	0.0021	0.0009
Chromium (Cr)	0.01	0.05	0.07	0.0478	0.0578
Copper (Cu)	0.001	0.002	0.005	0.0071	0.0089
Iron (Fe)	0.1	1.42	1.02	1.67	4.357
Manganese (Mn)	0.1	0.56	0.11	0.1139	0.2054
Molybdenum (Mo)	0.002	0.002	0.003	0.0008	0.004
Nickel (Ni)	0.03	0.04	0.06	0.0321	0.0472
Lead (Pb)	0.003	0.03	0.036	0.004	0.006
Strontium (Sr)	0.2	0.3	0.48	0.4907	0.5081
Vanadium (V)	0.008	0.009	0.01	0.01	0.01
Zinc (Zn)	0.002	0.02	0.3	0.1222	0.1408

^aThese data are compiled from previous works (10th of Ramadan city's Council, Embaby and El-Haddad 2007; DRC 2008)

Ni concentrations fluctuated from 0.0322 to 0.0472 mg/l, and Sr concentration fluctuated from 0.5081 to 0.588 mg/l. The results showed that bad treatment performance for all of the pond samples may be due to the accumulation of the sludge within the ponds together with the absence of proper dislodging. The total concentrations of Al, Cr, and Fe as high as 0.458, 0.0578, and 4.357 mg/l, respectively, were

recorded in oxidation pond no. 3, implying polluted pond (allowable limits are 0.2, 0.05 and 0.3 mg/l, respectively). A comparison of the three oxidation ponds indicated that the wastewater of oxidation pond no. 3 contains a higher total Zn, Mn, Cr, B, Al, Fe, Ni, and Pb concentrations than oxidation ponds no. 1 and no. 2, so oxidation pond no. 3 is considered the most polluted one. On the other side, the temporal variation of inorganic pollutant concentrations in the wastewater oxidation ponds shows significant annual fluctuations in the three ponds for all heavy metals concentration, but no specific trends could be identified.

Moreover, the measurements of organic pollutants BOD, COD, and TOC were higher than the permissible level, revealing to the intensity of pollution in the oxidation ponds (Table 6). The results of bacteriological analysis of eight samples of three oxidation ponds are shown in Table 7. Total colony counts of wastewater of oxidation ponds in all samples are generally high and range between 74 and 420×10^2 cfu/ml, this being generally higher than the recommended value (1×10^2 cfu/ml) for water. Recommended standard for water is nil, (FAO 1997). Also, the highest total coliforms counts were recorded in all the tested wastewater sampled range between 45 and 1600 MPN/100 ml. Recommended standard for water is less than 2 MPN/100 ml, TSI recorded the presence of E.coli or Klebsiella in samples 2, 3, 4, and 5 but Salmonella in sample 6, Shigella in sample 1 &

7, and both Salmonella and Shigella in sample 8. The presence of coliform group in most wastewater samples generally suggested that a certain of water samples may have been polluted with feces either of human or animal origin. Other more dangerous microorganisms could be present, (Richman 1997). The presence of enteric bacteria as reported in this study is an indication of the fecal pollution as a result of possible burst along pipelines or unhygienic handling of the water right from the treatment plant for tap water and borehole water. In this regard, (Umeh et al. 2005) reported the presence of enteric bacteria associated with fecal pollution, including *Escherichia coli*, *Shigella* sp., *Enterobacter aerogenes*, *Serratia* sp. and *Klebsiella* sp.

Groundwater pollution

It is important to note that the 10th of Ramadan city rests on the Pleistocene permeable sandstone formation that represents the most important groundwater aquifer in the Nile delta. The study of the groundwater pollution in the 10th of Ramadan city is mainly based on the results of the chemical inorganic analyses of water samples collected from the available drilled wells in the 10th of Ramadan city. Table 8 as well as the literature data is used to clarify the main different pollutants that were affected the groundwater quality. The wells ranged from 30 to 100 m in depth, following standard water sampling procedure, and were lined to ensure recharge from the screen of the wells only. The chemical analysis results showed that the groundwater samples have concentration of Al^{2+} , Fe^{2+} , and Si^{2+} ions higher than the acceptable levels of WHO (2011) standard. Moreover, the ion concentration of B^{2+} , Ba^{2+} , Cr^{2+} , Cu^{2+} , Mn^{2+} , Pb^{2+} , and Zn^{2+} in all groundwater samples were below the acceptable levels of WHO standard. It is clear that the groundwater samples had the same heavy metal pollutants in the oxidation ponds. This may be due to the precipitation of these pollutants from aeration in the oxidation ponds.

The biological pollutants in the groundwater samples in the study area were discussed through the measurements of

Table 6 Organic analysis of the wastewater oxidation ponds samples in 10th of Ramadan city. (El Sayed et al. 2012)

Sample no.	BOD	COD	TOC
1.	109.3	802	25.5
2.	102.3	472.5	297.7
3.	106.5	538	42.53
4.	88.8	472.5	34.02
5.	50.4	219.8	25.5
6.	73.5	263	34.2
7.	–	–	150
8.	–	–	133
Permissible limit	6	10	10

Table 7 Bacteriological analysis of representative samples in the 10th of Ramadan city. (El-Sayed et al. 2012)

Sample no.	Coliform count (M.P.N/100 ml)	Total colony count $\times 10^2$ (S.P.C/ ml at 37 °C)	Triple sugar iron (TSI)
1.	45	169	Shigella
2.	1800	420	<i>E. coli</i>
3.	110	74	<i>E. coli</i> or <i>Klebsiella</i>
4.	350	139	<i>E. coli</i> or <i>Klebsiella</i>
5.	1800	360	<i>E. coli</i> or <i>Klebsiella</i>
6.	900	213	Salmonella
7.	275	85	Shigella
8.	1600	146	Shigella, Salmonella

Table 8 Concentrations of heavy metals of groundwater samples from the selected eight locations in the 10th of Ramadan city expressed in mg/l. (During 2010, 2012)

Parameter	Recommend conc. (mg/l) (WHO 1996a, 2011)	(S1) Dec-10	(S2) Dec-10	(S3) Dec-10	(S4) Dec-10	(S5) Jul-12	(S6) Jul-12	(S7) Jul-12	(S8) Jul-12	Average
pH		7.6	6.5	6.1	6.2	7.1	6.9	6.9	7.1	6.8
E.C.		2400	4310	1035	6400	8280	10,930	20,060	7640	7631.875
TDS		1536	2785	6624	4096	5161	7035	12,438	4774	5556.125
NO ₃	11	38	54.2	100	76.4	21	52.4	46.5	58.1	55.825
PO ₄	1	0.0825	0.2098	0.2935	0.1478	0.14	0.05	0.44	2.1	0.43295
Al	0.2	0.109	0.1756	0.6249	0.3232	<0.03	0.0438	0.2776	0.8609	0.301875
B	1	0.4522	1.028	2.22	0.4837	0.6513	0.4722	0.4201	0.506	0.779188
Ba	2	0.061	0.0721	0.0469	0.0292	0.0785	0.1685	0.2088	0.0775	0.092813
Cd	0.003	<0.0007	<0.0007	<0.0007	<0.0007	<0.0006	<0.0006	<0.0006	<0.0006	BDL
Co	<0.05	<0.001	<0.001	<0.001	<0.001	<0.0007	<0.0007	<0.0007	<0.0009	BDL
Cr	0.05	<0.01	0.0263	<0.01	<0.01	0.0215	<0.01	<0.01	<0.01	0.005975
Cu	1	<0.003	<0.003	0.0092	0.0057	<0.009	<0.009	0.0332	0.0286	0.009588
Fe	0.3	0.0405	0.0486	0.1145	0.0625	<0.02	0.207	2.633	0.7488	0.481863
Mn	<0.1	<0.003	<0.003	0.0098	0.0065	<0.005	0.0322	0.0578	0.0864	0.024088
Mo	0.05	0.0019	<0.0008	<0.0008	<0.0008	<0.004	<0.004	<0.004	<0.004	BDL
Ni	0.01	<0.001	0.0021	0.0038	0.0033	<0.001	<0.001	<0.001	<0.001	0.00115
Pb	0.01	0.0064	0.0071	<0.004	0.0051	<0.006	<0.006	<0.006	0.0144	0.004125
Sr	0.11	1.985	2.309	10.06	5.94	4.696	10.14	20.36	7.721	7.901375
V	0.01	<0.01	<0.01	<0.01	<0.01	<0.01	<0.01	<0.01	<0.01	BDL
Zn	3	<0.001	<0.001	0.1338	0.0564	<0.0008	<0.0008	0.2085	0.1314	0.066263

nitrate compounds and phosphate content (Table 8). The excess usage of inorganic fertilizers containing nitrogen is the main source of nitrate soluble in water, which results in a high availability for plants. About 30% of these salts are absorbed by plants and the rest go into solution with drainage water. Consequently, nitrate ion can easily reach the groundwater through the soil from nitrogen fertilizers because adsorption to the soil is very low (Menció et al. 2016). The results of the biological analyses indicated that the concentrations of nitrate ions in some groundwater samples are greater than the acceptable limit. On the other hand, groundwater samples cannot be considered polluted with phosphate.

The bacteriology analyses showed that the total colony counts of groundwater in the east of the city are generally high and ranged between 69 and 234 × 10² cfu/ml (Table 9). This considers generally higher than the recommended value (1 × 10² cfu/ml) for water (FAO 1997) and gave total colony counts low in the west of the city. The total coliforms counts recorded for testing groundwater samples were 110 MPN/100 ml; recommended standard for water is less than 2 MPN/100 ml. The bacteriology analyses and microbial contamination test revealed that the sample 2 contaminated with coliform in the east of the city. On the other hand, the groundwater samples in the west of the city recorded the absence of Coliforms group and enteric bacteria. The triple sugar iron (TSI) reaction recorded the presence of

Table 9 Bacteriological analysis of well samples in the 10th of Ramadan city. (After El Sayed et al. 2012)

Sample no.	Location	Coliform count (M.P.N./100 ml)	Total colony count × 10 ² (S.P.C/ml at 37 °C)	Triple sugar iron (TSI)
Sample 1	East of city	–	82	–
Sample 2	East of city	110	234	Salmonella
Sample 3	East of city	–	69	–
Sample 4	East of city	–	74	–
Sample 5	west of city	–	18	–
Sample 6	west of city	–	25	–
Sample 7	west of city	–	20	–
Sample 8	west of city	–	13	–

Salmonella in sample 2 which may be the main source for Taifud fever and food contamination. The bacteriology analyses explain the effect of the bacteriology contamination to the groundwater in the east of the city due to the leakage of the ponds to it.

Models of groundwater flow

Groundwater modeling such as MODFLOW has become a very useful and established tool to study problems of groundwater quality and management and also to predict the future behavior of an investigated aquifer system. Pollutant transport models simulate the movement and chemical alteration of pollutants as they move through the subsurface. The model simulates the pollutant movement by advection, diffusion, and dispersion. The outputs from model simulations are pollutant concentrations that are in equilibrium with the groundwater flow system and in geo-chemical conditions in the modeled area (Dawoud et al. 2014).

This software consists of input, run, and output sections. In first section, characteristics of soil and groundwater and also boundary condition is assigned for software. Run section is designed to translate an input section in the standard input to simulate. Output illustrates the results of simulation included concentration of pollution, water level and so on. It uses the cell-by-cell data which is computed and outputted to establish the results. These models gained wide acceptance because they are well documented, validated, and verified.

Conceptual model of the water flow system is constructed to the Quaternary unconfined aquifer (Fig. 4) which consists of one complex layer that is composed mainly of coarse to fine sand with dominance of clay lenses intercalation zones. Figure 4 illustrates a two dimensional model (one vertical layer). The unconfined aquifer is characterized by lateral and

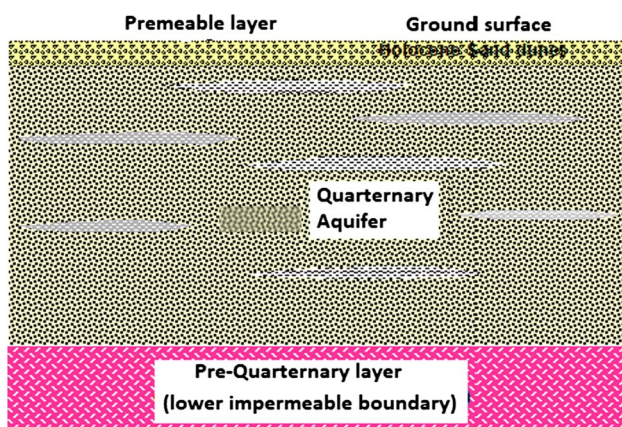


Fig. 4 Conceptual model of a two dimensional model (one vertical layer) Quaternary unconfined aquifer in the 10th of Ramadan city area

vertical facies changes with thickness varied from one place to another.

The chemical results demonstrated that there was an excessive limit of three metals such as aluminum Al^{2+} , iron Fe^{2+} , and strontium Sr^{2+} . The assessment process on the concentration of aluminum, iron, and strontium would be important to know the amount of spreading of pollution in the future. It might be helpful to control pollution from oxidation ponds in the study area.

Groundwater flow model design

The visual MODFLOW v.4.2 code was selected to model the groundwater flow in the Quaternary aquifer. It can simulate steady and transient flow in an irregularly shaped flow system in which aquifer layers can be confined, unconfined, or a combination of them.

The first step of the groundwater flow model design is generating a suitable groundwater flow model grid, which, has to be well adjusted to the model domain. The computational grid for the aquifer domain in the studied Quaternary aquifer is divided into 1500 cells (50 columns and 30 rows). The dimensions of the cell nodes equal $1.0 \text{ km} * 1.0 \text{ km}$ (Fig. 5).

Various data from different sources were assigned to the grid for the groundwater flow model design that includes a boundary condition that assumed to be a constant head boundary from north (Ismailia canal), the general head boundary of the South, constant head boundary from the east (Suez Canal) and no flow boundary from west. Bulk density and effective porosity were collected from (Shata 1978), specific yield, storage coefficient, transitivity, horizontal and vertical hydraulic conductivities from the analysis of available pumping test (Table 1, Gad 1995; Ismail 2008; Gad et al. 2015). El-Mahsama Lake and oxidation ponds were entered as a lake feature, using field measurement depth (3 m), discharge, an annual recharge rate of 14 mm/year, and an annual evapotranspiration rate of 2920 mm/year (13 meteorological stations, Ismail 2008). The Ismailia canal was added as a river boundary using an average depth of 4 m (Gad et al. 2015). Top and bottom elevations of the aquifer layer derived from DEM files (digital elevation model) are available from the World Wide Web (<http://www.emrl.byu.edu/gsda>) to automatically delineate the ground surface elevation above sea level. The values of the top layer matrix extracted through the use of DEM file are processed by surfer software and saved as spreadsheet file accepted by the Visual MODFLOW package. On the contrary, due to the lack of bottom layer elevation data and depending on the few well logs data referring to an aquifer average saturated thickness 140 m, the bottom layer elevation map of Quaternary aquifer was obtained by subtracting a constant value of

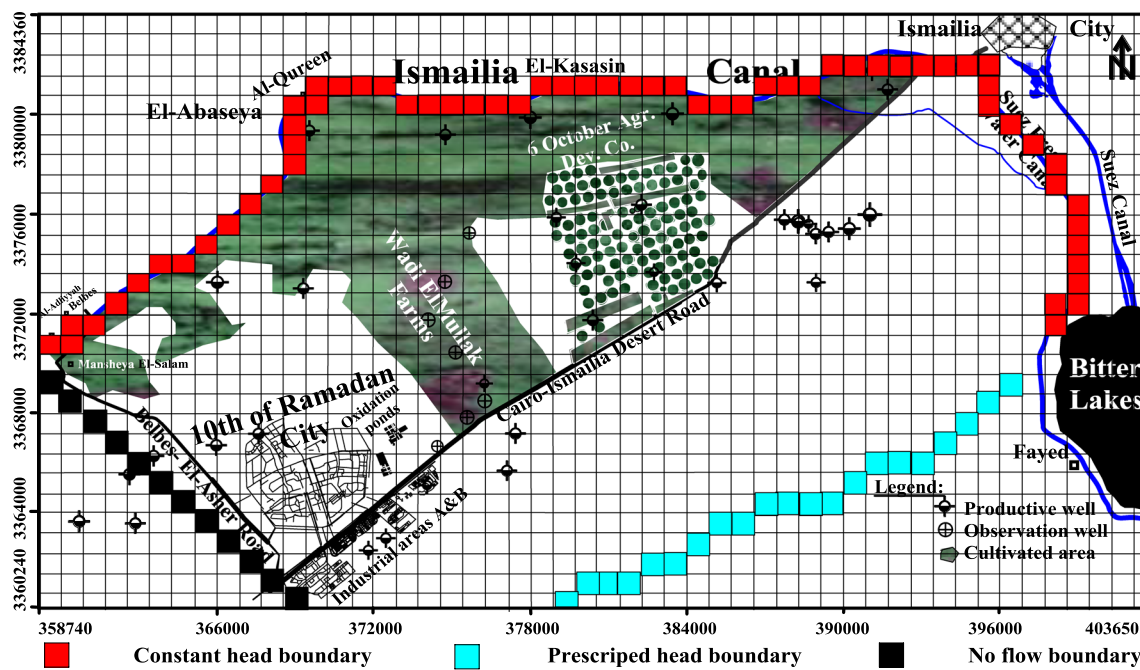


Fig. 5 Model domain grid and the boundary conditions of the simulated Quaternary aquifer. (ELnemr et al. 2015)

140 m from the top layer elevation data matrix using surfer software to reprocess the resulted map through visual MODFLOW software. The initial hydraulic head is the distribution of head in the groundwater system at the start of the simulation (Anderson and Woessner 1992). Initial hydraulic heads distribution in the Quaternary aquifer during Dec. 1992 (Gad 1995) was obtained from the well database in the study area. The ground elevations extracted from the corrected DEM of the area at each model cell are used, and then depth to static water level values from the well database are subtracted from each DEMs obtained. The results of this calculation are used as initial prescribed hydraulic heads in each cell for the initial specification of head values. MODFLOW was set to 10,950 days (30 years approximately) to represent the total time for prediction.

The governing equations of the groundwater flow are derived by mathematical combination between the water balance equation and Darcy's law (Anderson and Woessner 1992). The groundwater flow can be described in 3D under non-equilibrium conditions in a heterogeneous and anisotropic medium using the following equation; (Bear and Verruijt 1987)

$$\frac{\partial}{\partial x} \left(K_x \frac{\partial h}{\partial x} \right) + \frac{\partial}{\partial y} \left(K_y \frac{\partial h}{\partial y} \right) + \frac{\partial}{\partial z} \left(K_z \frac{\partial h}{\partial z} \right) \pm W = S \frac{\partial h}{\partial t} \quad (1)$$

where K_{xx} , K_{yy} , and K_{zz} are the values of hydraulic conductivity along the x , y , and z coordinate axes, h is the hydraulic head, W is a volume flux per unit volume (a positive sign for

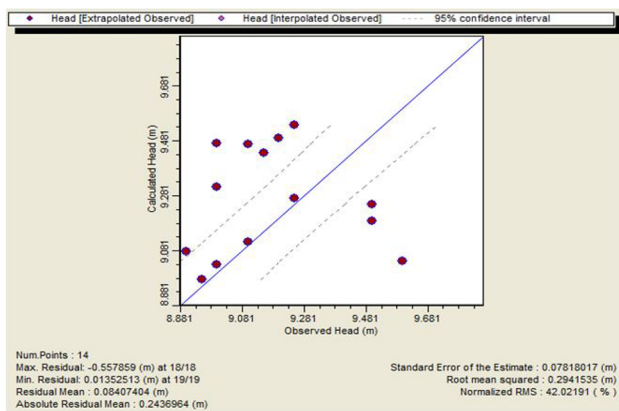
the inflow and negative sign for the outflow), and S is the specific storage or specific yield and t is time.

Models should be calibrated and verified by adjusting the values of the different hydrogeological properties to reduce any disparity between the simulated (calculated) results and field (measured) data. The calibration for hydraulic head in the Quaternary aquifer was obtained from two synoptic water level surveys conducted on Dec. 1992, by Gad (1995) and on Dec. 2005, by Gad et al. (2015), Figs. 2, 3. This data set was chosen for the quantitative comparisons of the simulated versus measured head because it included all of the wells that are important to the transport simulations within the study area.

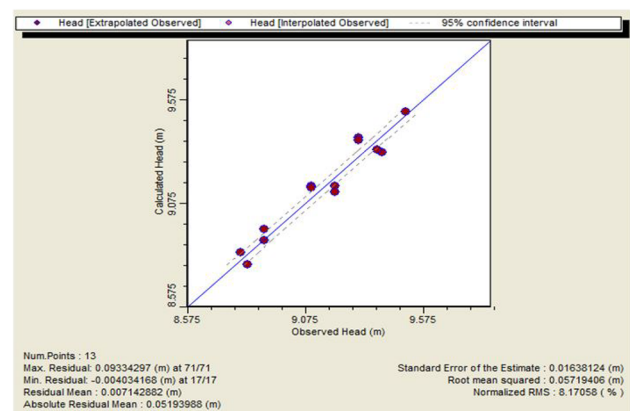
For the calibrated groundwater flow model, the mean error (ME) between simulated and measured head for the 14 wells listed was -0.19 m, the mean absolute error (MAE) was 0.2439 m, and the root-mean-squared error (RMSE) was 0.0.2941 m. Measured head in the calibration data set (Table 10) ranges from 8.8976 m in well no. 1 to 9.9976 m in well no. 3. The normalized RMS appears as 42.02% before calibration (Fig. 6a) which indicates the great difference between the heads calculated by the model and actually measured heads during the year of 1992 so, the calibration process is very important to minimize this normalized RMS to a lower possible value. After many times of changing the hydraulic conductivity (k) value and canceling an observation well, the normalized RMS between the observed and simulated heads was minimized to 8.17% and the calculated head is very closely related

Table 10 Measured and simulated head in 14 observation wells of Quaternary aquifer (steady state)

S. no.	Steady-state conditions							
	Before calibration				After calibration			
	Measured head (m)	Simulated head (m)	Absolute difference	RMS	Measured head (m)	Simulated head (m)	Absolute difference	RMS
1.	8.8976	9.081	0.1834	0.0336356	8.8	8.825	0.025	0.000625
2.	9.9476	9.981	0.0334	0.0011156	8.825	8.775	-0.05	0.0025
3.	9.9976	9.031	-0.9666	0.9343156	8.9	8.9	0	0
4.	9.997	9.314	-0.683	0.466489	8.9	8.95	0.05	0.0025
5.	9.997	9.464	-0.533	0.284089	9.1	9.15	0.05	0.0025
6.	9.241	9.106	-0.135	0.018225	9.2	9.125	-0.075	0.005625
7.	9.241	9.106	-0.135	0.018225	9.2	9.175	-0.025	0.000625
8.	9.297	9.431	0.134	0.017956	9.275	9.375	0.1	0.01
9.	9.1976	9.481	0.2834	0.0803156	9.275	9.4	0.125	0.015625
10.	9.281	9.264	-0.017	0.000289	9.375	9.35	-0.025	0.000625
11.	9.281	9.531	0.25	0.0625	9.375	9.35	-0.025	0.000625
12.	9.497	9.197	-0.3	0.09	9.4	9.3	-0.1	0.01
13.	9.497	9.247	-0.25	0.0625	9.475	9.5	0.025	0.000625
14.	9.597	9.047	-0.55	0.3025				



(a)



(b)

Fig. 6 Calculated head and the observed head for the steady-state condition **a** before calibration, **b** after calibration

to the field observed head after calibration (Table 10 and Fig. 6b). In addition, the calibration procedure for the constructed model for unsteady-state condition is carried out based on the last mentioned steps.

In the process of calibration of transient state, the calibrated groundwater levels of the year 1992 resulting from the steady-state simulation are used as starting head to the transient calibration stage in order to reach the field groundwater levels that recorded in 2005 (Gad et al. 2015) so, specific yield values were modified on a trial and error basis, until a good match between the observed heads of years 1992 and 2005 and the calculated heads were achieved (Table 11). It can be seen, in general, that there is good agreement between

the observed and simulated head as normalized RMS value changed from 37.85 to 7.33% (Fig. 7a, b).

After completing the calibration process, the heads resulting from the unsteady-state simulation are used as starting heads to predict the future expansion of the pollution plume. The developed model is run for every year during the stress period (2005–2035). For every proposed time step, the above step will be repeated before running the model, noting that the difference will be appearing in each time.

The solutions obtained for the simulation model in this study appear to be insensitive to the boundary conditions. The fact that both pumping scenarios yielded similar output in terms of flow direction and head distribution lends

Table 11 Measured and simulated head in 9 observation wells of Quaternary aquifer (unsteady state)

Unsteady-state condition				
Before calibration			After calibration	
Observed	Calculated		Observed	Calculated
1.	8.8976	9.181	8.825	8.825
2.	8.9476	9.031	8.9	8.925
3.	9.013	9.3476	9.1	9.2
4.	9.0976	9.181	9.2	9.175
5.	9.1476	9.4476	9.2	9.225
6.	9.2476	9.3476	9.3	9.4
7.	9.2476	9.5476	9.375	9.325
8.	9.4976	9.281	9.5	9.525
9.	9.4976	9.331		

credence to the modeling approach used in this study. Although the model may misrepresent the flow system near the model boundaries, the calibrated model provides a reasonable approximation of the three-dimensional groundwater flow system in the vicinity of the pollution plume and extraction wells.

The results of the simulation process (Figs. 8, 9, 10) show the predicted hydraulic head after time of simulation of 10, 20, 30 years

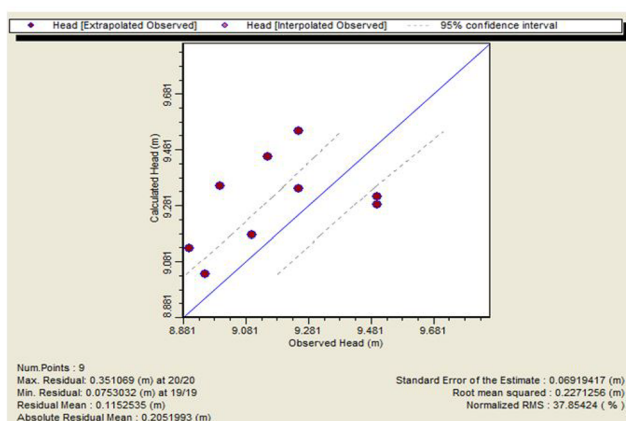
The groundwater flow direction is directed mainly from south to north direction (regional flow) with low hydraulic gradient. An opposite flow direction is observed from north to south direction where Ismailia canal represents the main recharging source for the Quaternary aquifer. The predicted groundwater flow direction based on the model result shows to concentric directions in case of the resulted cone of depressions in the low eastern areas and in the cultivated areas north the 10th of Ramadan city. As a result of high

discharge, there are two cones of depression in the northeast and west direction and still increase over 10, 20, 30 years. In addition, the water table contours (equipotential lines) show a general trend more or less parallel to the Ismailia canal. Moreover, their latitudes decrease as they go far from it. This indicates that Ismailia canal represents a recharge front for the Quaternary deposits, and it is considered the main factor of recharge as same as a Suez freshwater canal. The groundwater levels in this area are always lower than the surface water level in Ismailia canal and other irrigation canal, indicating influent conditions around the eastern drainage natural systems. On the other hand, it is noticed that the northeastern areas are appearing as an open trench with flow from all directions towards the central low-lying areas due to the concentration of wells in these parts with heavy uncontrolled flow. Far from the over-pumping locations, the contour line configuration is almost without notable changes.

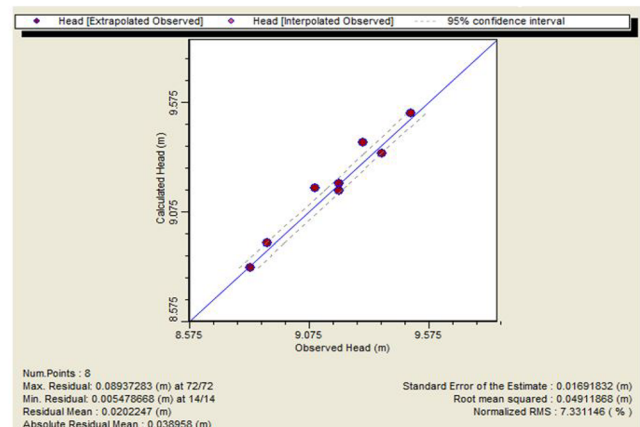
A numerical pollutant transport model

Simulation of soluble pollution migration by computer is a way to cover the hiatus between field observations and characteristic water movement in porous media. MT3DMS (Zheng 2006) was also interfaced with MODFLOW to solve groundwater pollution. Along with such process, it also possible to monitor and follow the pollutants which exist in groundwater or infiltrated from surface sources by lateral and/or vertical migration.

They generally move with the groundwater flow in the aquifer. As pollutant moves, it disperses. This means that its concentration decreases as it moves far away from the source of the pollution. For this reason, there is different concentration of pollutants at different points in the aquifer. The representation of these different concentrations is called pollutant plume. The looking of the plume depends on the



(a)



(b)

Fig. 7 Calculated head and the observed head for the unsteady-state condition **a** before calibration, **b** after calibration

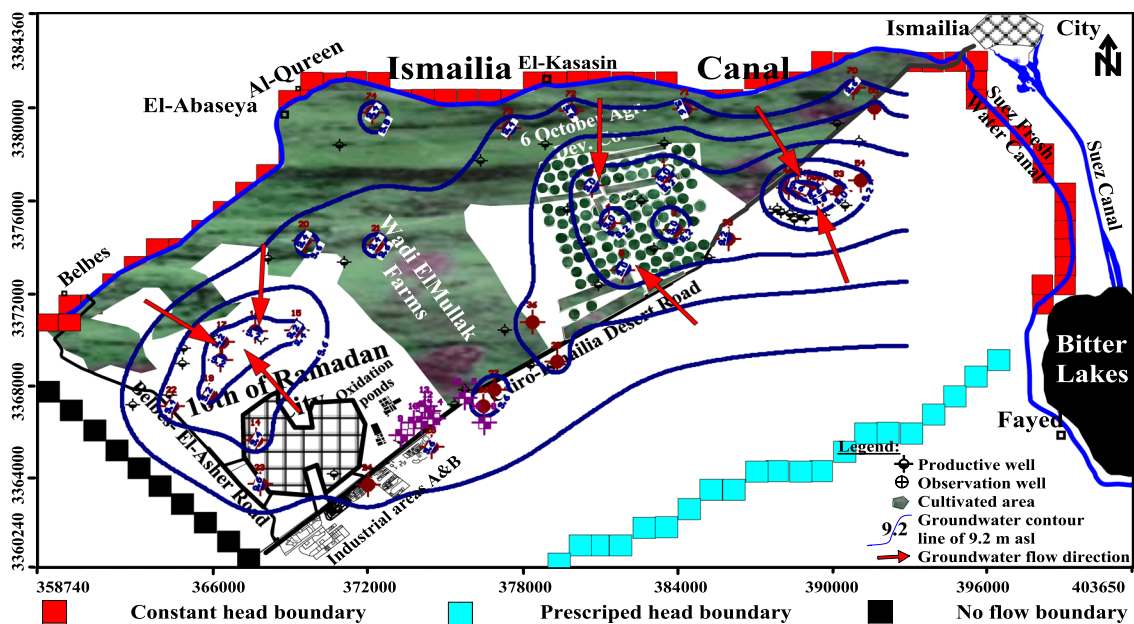


Fig. 8 Predicted head after 10 years of the simulation in Quaternary aquifer

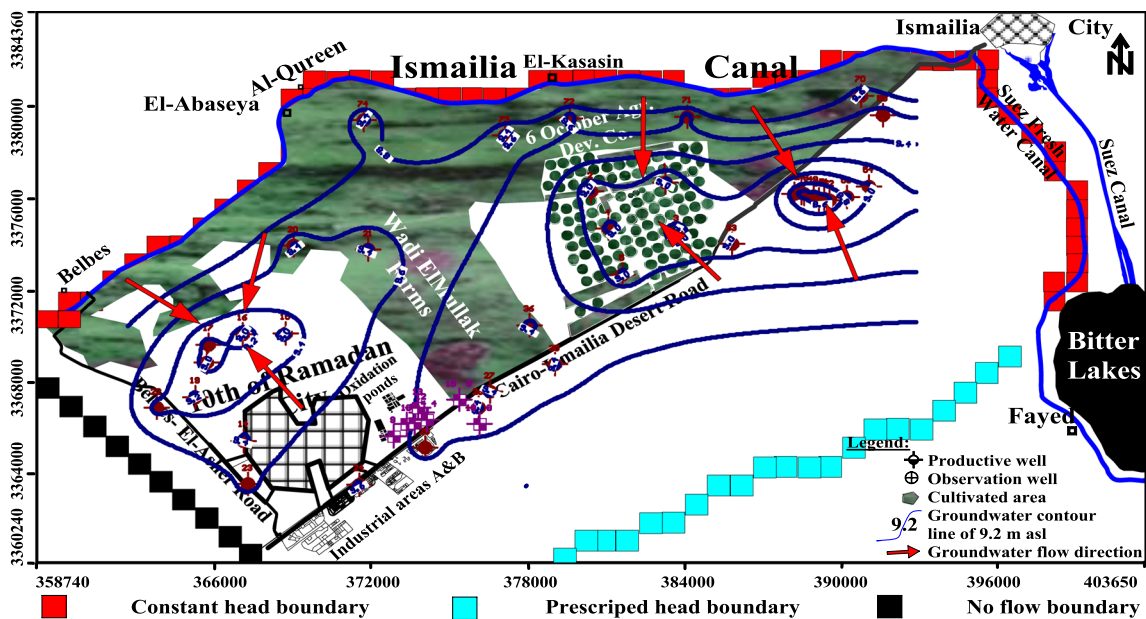


Fig. 9 Predicted head after 20 years of the simulation in Quaternary aquifer

specific contaminants, the type of contamination source, different soils in the study area and where the aquifers are located. When talking about pollutants movement, it is also very important to talk about the area affected by the spreading of groundwater pollutant. A pollutant may be appeared into groundwater for only a short time and very small area, but as it disperses the pollutant can affect a very large area. The boundary concentration was assigned to the model for

the main three concentrations Al, Fe, and Sr in ponds 1, 2, and 3 for the year 2005 and 2010 which based on analysis tests of water samples from the ponds. The assigned constant concentration of Al equals 0.15, 0.20, and 0.5 mg/l for pond 1, 2 and 3 respectively, for the year 2005 and equals 0.517, 0.219, and 0.695 mg/l for the year 2010. Pond 1, 2 and 3 were assigned a constant concentration of Fe equals 0.17, 0.24, and 1.42 mg/l for the year 2005 where equals 0.552,

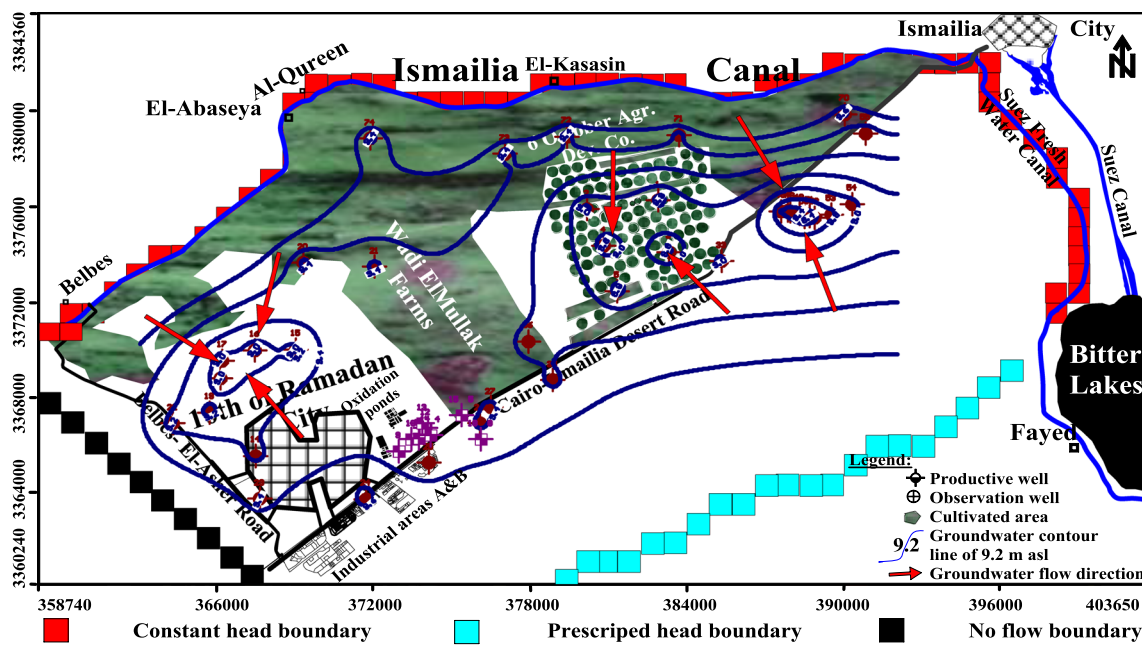


Fig. 10 Predicted head after 30 years of the simulation in Quaternary aquifer

0.215, and 1.67 mg/l for the year 2010. Here Pond 1, 2, and 3 were assigned a constant concentration of Sr equals 0.55, 0.30, and 0.30 mg/l for the year 2005 and equals 0.581, 0.526 and 0.491 mg/l for the year 2010. The initial concentration of the aquifer was assigned to be equal 0.23, 0.10, and 1.13 mg/l for Al, Fe, and Sr, respectively. In this study, the proposed model is a non-reactive transport simulation in this study area.

For movement of a non-reactive solute or pollutant in groundwater regime, the condition of mass balance of the solute should also be satisfied. The mathematical equation describing this process may be expressed as:

$$\frac{\partial}{\partial x} \left(D_x \frac{\partial C}{\partial x} \right) + \frac{\partial}{\partial y} \left(D_y \frac{\partial C}{\partial y} \right) + \frac{\partial}{\partial z} \left(D_z \frac{\partial C}{\partial z} \right) - \frac{\partial}{\partial x} (C V_x) + \frac{\partial}{\partial y} (C V_y) + \frac{\partial}{\partial z} (C V_z) - \frac{C_0 W}{\mu_e} = \frac{\partial C}{\partial t} \quad (2)$$

where V_x , V_y , and V_z are the velocity components of groundwater along the three coordinate axes, C is the solute concentration at any point, D_x , D_y , and D_z are the principal components of the dispersion coefficient, μ_e is the effective porosity and C_0 is the concentration of the solute in the source or sink.

Because of the high absorption capacity of the soil for adsorption of Al, Fe and Sr, they cannot leach or move with groundwater in a short time (Khan and Ansari 2005). The periods of pollutants migration prediction were selected different years (10, 20, and 30 years) to obtain the distinctive

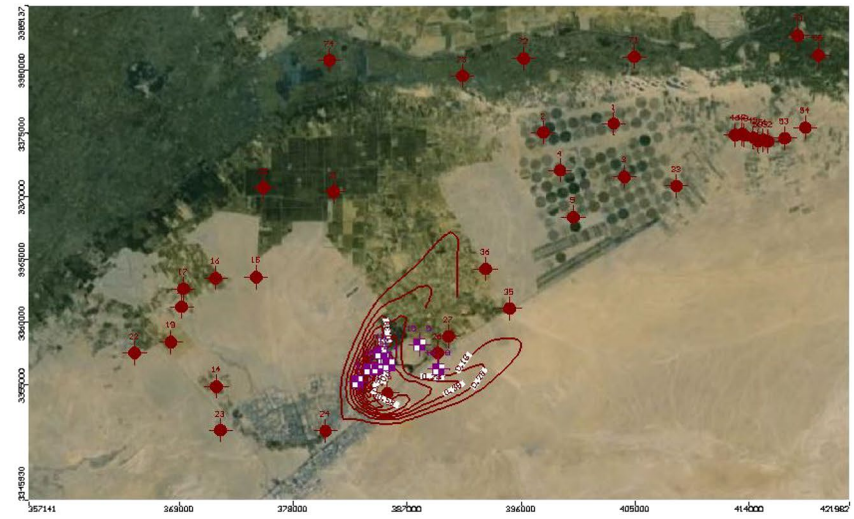
results and approving mobility of overloaded Al, Fe, and Sr within the longer time in the study area. This enables the groundwater carried pollutants to bypass the soil pores which permit migration of high concentration of them through the soil (Knapp and Hardy 2002; Saghravani and Mustapha 2011).

From Figs. 11, 12, and 13 for Al, Fe, and Sr which represent the pollutant movement in the study area, it is noticed that the pollution is coming from oxidation ponds. The groundwater is moving towards Wadi El-Mollak area and Six October Agriculture Company. The areas will be affected by pollution are Six October Agriculture Company, El Shabab canal and Wadi El-Mollak area. On the other hand, there is lateral flow starting after 20 years that threatens a great part of the city.

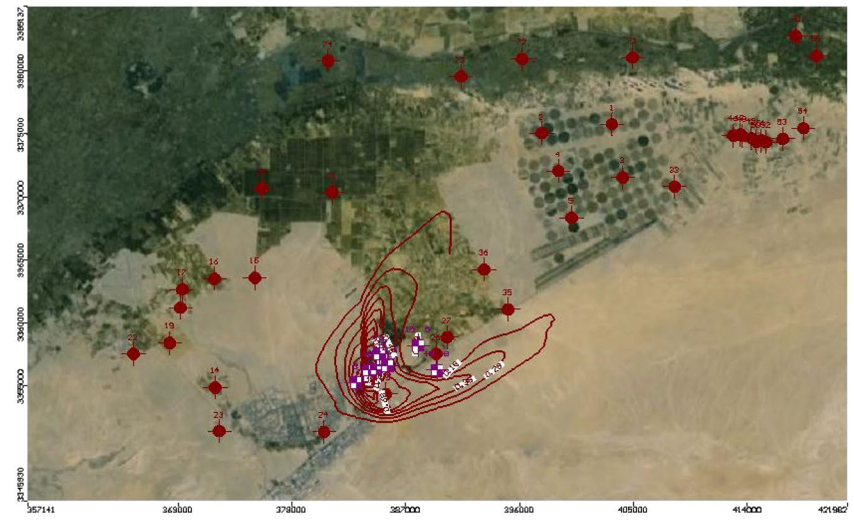
The pollution traveled at different distance as mentioned in (Table 12, Fig. 11a–c) which represents the Al pollutant, and it is seen that after 10 years the plume of the pollutant reached 16.5 km, and after 20 years, it reached 18.0 km with increase in distance about 1.5 km and after 30 years, and it is still 18.0 km without change in distance. Also from (Fig. 11a–c), it is clear that the plume of the pollutant reached 15 km from the starting point in SE direction after 10 years, and after 20 years, it reaches 19.6 km with increase of about 4 km, and in addition, it reached 21.0 km with an increase of about 2.4 km after 30 years.

According to (Fig. 12a–c) which represents Fe pollutant, it is shown that after 10 years the plume length reached 18 km from the starting point in a NE direction. After 20 years, it reached 19.8 km with an increase of about

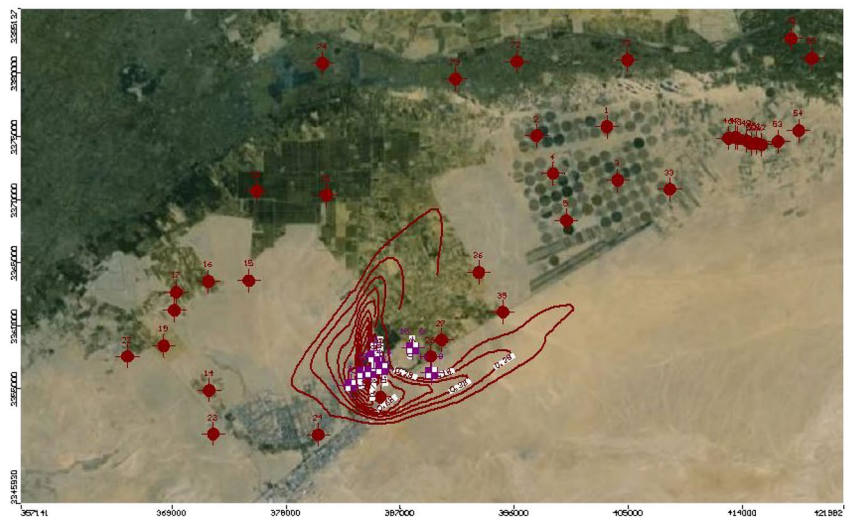
Fig. 11 Al pollutant transport **a** after 10 years, **b** after 20 years, and **c** after 30 years



(a)

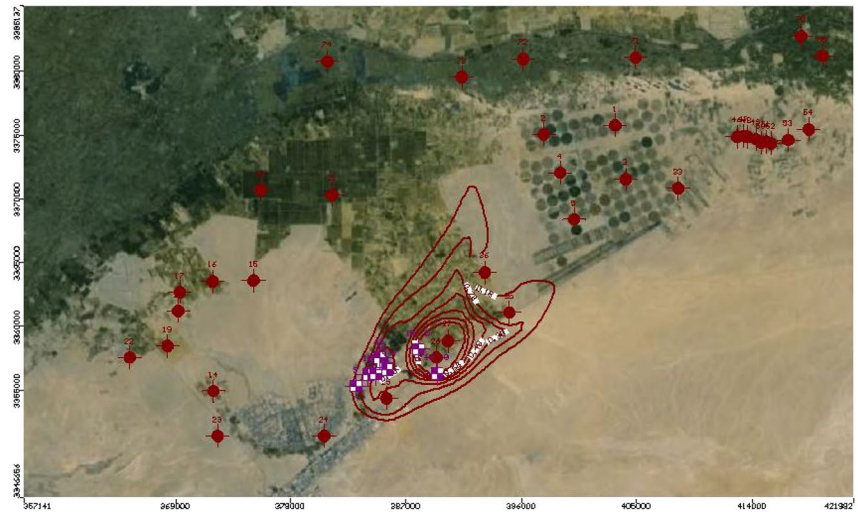


(b)

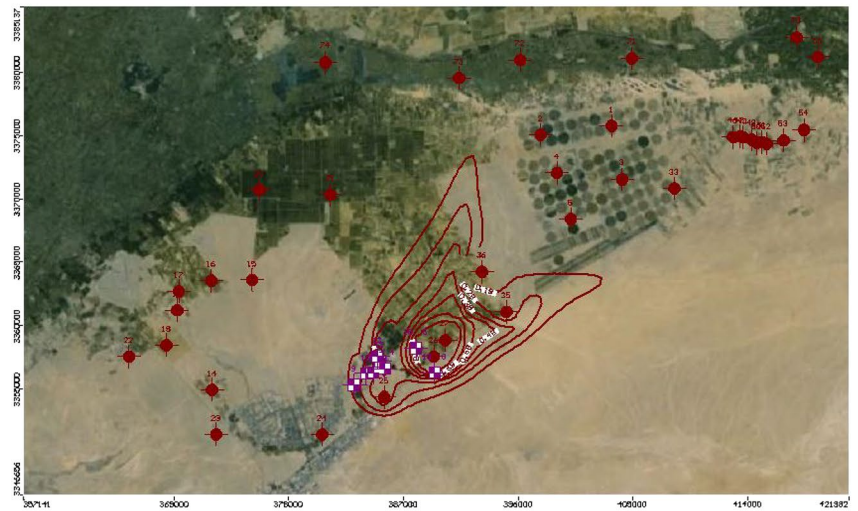


(c)

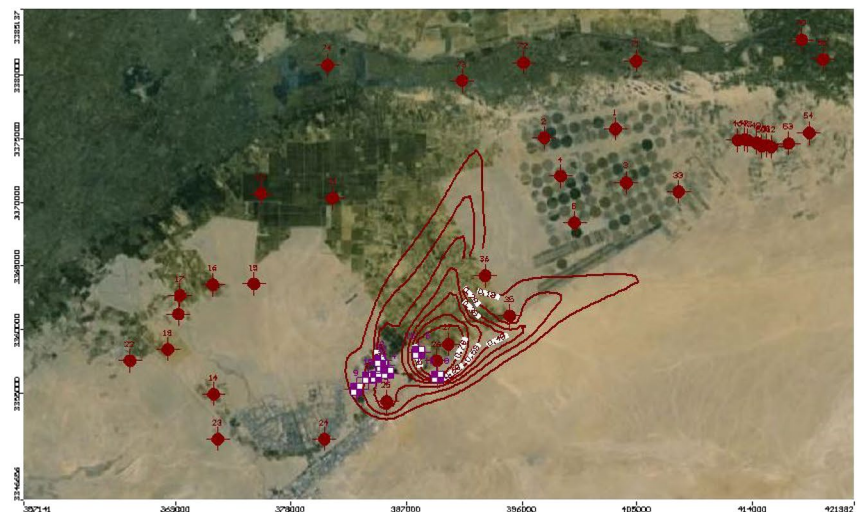
Fig. 12 Fe pollutant transport **a** after 10 years, **b** after 20 years, and **c** after 30 years



(a)

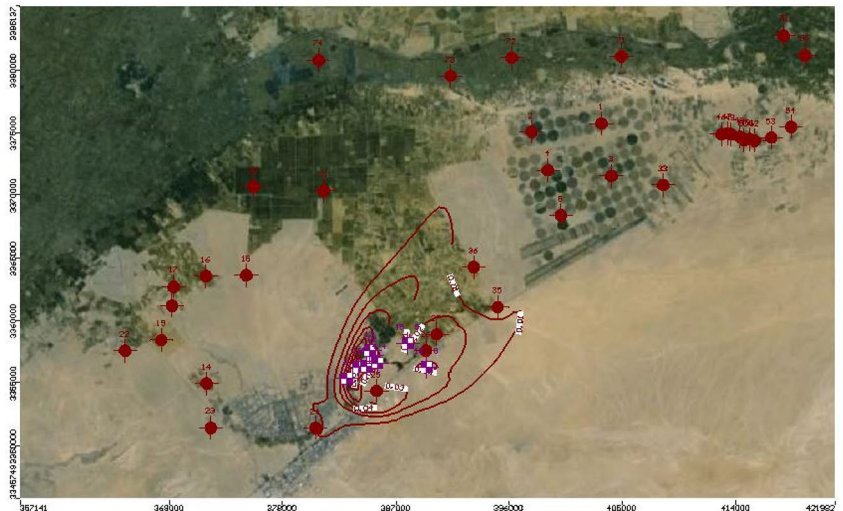


(b)

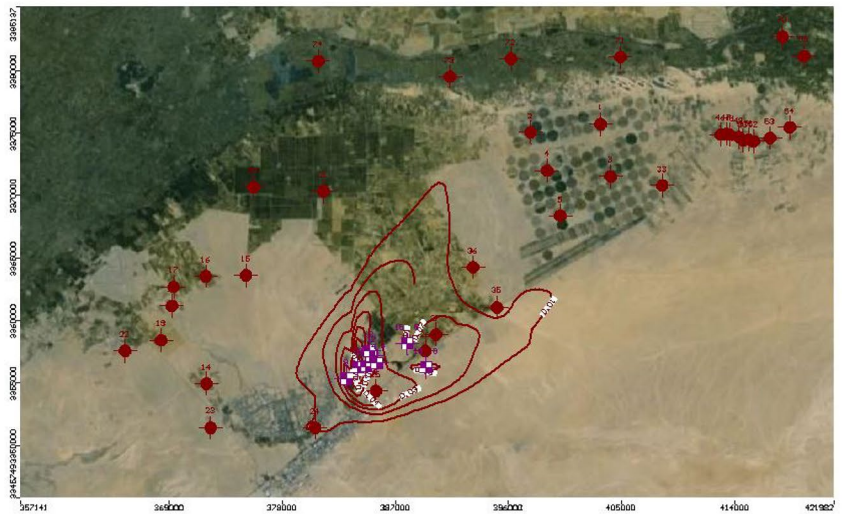


(c)

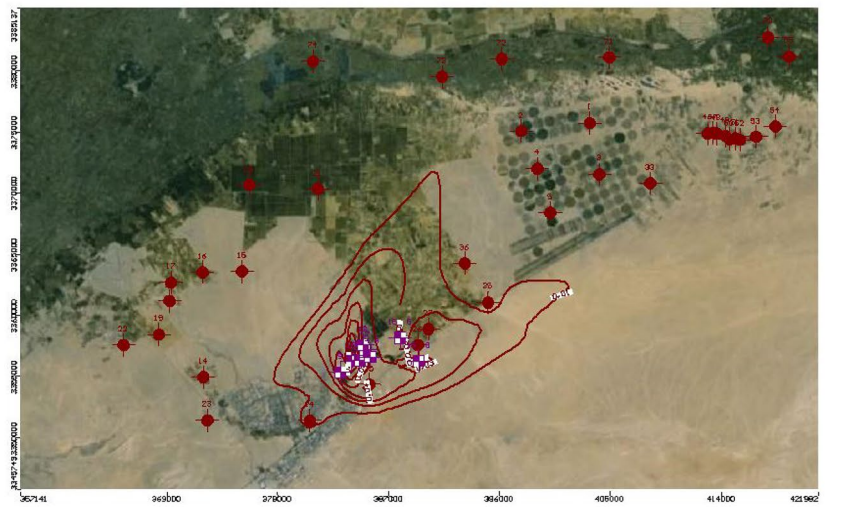
Fig. 13 Sr pollutant transport **a** after 10 years, **b** after 20 years, and **c** after 30 years



(a)



(b)



(c)

Table 12 Predicted transport distance of contaminant plume based on the results of MT3D model

Time (year)	NE			SE		
	Length of plume	Distance (m)		Length of plume	Distance (m)	
Al						
After 10 years	5.5	16.5	1500	5	15	1800
After 20 years	6	18.0	900	6.2	19.6	2400
After 30 years	6	18.0	0	7	21.0	2400
Fe						
After 10 years	6	18	1500	5.4	16.2	1200
After 20 years	6.6	19.8	600	6.5	19.5	1500
After 30 years	6.8	20.4	600	7.5	22.5	3000
Sr						
After 10 years	6.7	20.1	1800	6.1	18.3	1800
After 20 years	7.3	21.9	900	7.1	21.3	1800
After 30 years	7.6	22.8	900	8	24	900

1.8 km. After 30 years, it reached 20.4 km with an increase of about 600 m. Also from (Fig. 12a–c), it is clear that the plume of the pollutant reached 16.2 km from the starting point in SE direction. After 20 years, it reached 19.5 km with an increase of about 2.7 km. After 30 years, it reached 22.5 km with an increase of about 3 km.

According to (Fig. 13a–c) which represents the Sr pollutant, after 10 years the plume of the pollutant reached 20.1 km from the starting point in a NE direction. After 20 years, it reached 21.9 km with an increase of about 1.8 km. After 30 years, it reached 22.8 km with an increase of about 900 m. Also from (Fig. 13a–c), it is clear that the plume of the pollutant reached 18.3 km from the starting point in SE direction. After 20 years, it reached 21.3 km with an increase of about 3 km. After 30 years, it reached 24.0 km with an increase of about 2.7 km.

Conclusions and recommendations

The chemical analysis results referred that some of pollutants in the oxidation ponds exceeded the standard limit such as Al^{3+} , Fe^{2+} , Sr^{2+} , Cr^{2+} , and Ni^{2+} which were attributed to both industrial effluents and domestic sewage. Therefore, the water of the oxidation ponds was not suitable for irrigation of plants purpose since it reflects critical environmental risks. Also the results show that the groundwater samples contain high concentrations of Al^{3+} , Fe^{2+} , Sr^{2+} than the WHO (2011) acceptable limit. The results of the groundwater flow and transport simulation reveal the expansion of pollution plume. It travelled 18, 20.4 and 22.8 km due NE direction after 30 years of simulation for Al^{3+} , Fe^{2+} , Sr^{2+} pollutants, respectively. The results explained that the water of oxidation ponds must not use for irrigation purpose without treatment process to eliminate the high concentration of the predicted

pollutants. The study gave a sound alarm to make new drilled wells far away from pollution sources and several observation wells should be installed around oxidation ponds for periodic monitoring.

The 10th of Ramadan city factories should not discharge its industrial effluents to water sources without treatment and wastes from oxidation ponds must not be used in irrigation.

New drilled wells should be located far away from pollution sources and observation wells should be installed around oxidation ponds for periodic monitoring.

The spatial and temporal variations suggest that the scale and collect samples require careful planning, and a single sample may not be give a satisfactory evaluation of the levels of heavy metal pollution in the oxidation ponds ecosystems.

Open Access This article is distributed under the terms of the Creative Commons Attribution 4.0 International License (<http://creativecommons.org/licenses/by/4.0/>), which permits unrestricted use, distribution, and reproduction in any medium, provided you give appropriate credit to the original author(s) and the source, provide a link to the Creative Commons license, and indicate if changes were made.

References

- Abu El Ela AI (2008) Environmental impact of the oxidation ponds of the industrial area of 10th of Ramadan city, Egypt. Master thesis, Faculty of science, Mansoura University, Egypt
- Abu-El-Sha'r WY, Hatamleh RI (2007) Using MODFLOW and MT3D Groundwater flow and transport models as a management tool for the Azraq groundwater system. *Jordan J Civil Eng* 1(2):153–172
- Anderson MP, Woessner WW (1992) Applied groundwater modeling: simulation of flow and advection transport. Academic Press, San Diego, p 318
- Attwa M, Gemail K, Eleraki M, Zamzam S (2013) Assessment of oxidation ponds impact using DC resistivity method in Tenth of Ramadan city, Egypt. In: The 20th international geophysical

- congress and exhibition of Turkey, Antalya, Turkey, 25–27 November 2013
- Ayvaz MT (2016) A hybrid simulation–optimization approach for solving the areal groundwater pollution source identification problems. *J Hydrol* 538(2016):161–176
- Banejad H, Mohebzadeh H, GhobadI MH, Heydari M (2014) Numerical simulation of groundwater flow and contamination transport in Nahavand Plain Aquifer, West of Iran. *J Geol Soc India* 83:83–92
- Bear J, Verruijt A (1987) Modeling groundwater flow and pollution. D. Reidel Publishing Company, Dordrecht, p 414
- Chintalapudi P, Pujar P, Khadse G, Sanam R, Labhasetwar P (2017) Groundwater quality assessment in emerging industrial cluster of alluvial aquifer near Jaipur, India. *Environ Earth Sci* 76:8
- Datta B, Petit C, Palliser M, Esfahani HK, Prakash O (2017) Linking a simulated annealing based optimization model with PHT3D simulation model for chemically reactive transport processes to optimally characterize unknown contaminant sources in a former mine site in Australia. *J Water Resour Prot* 9:432–454
- Dawoud WA, Negm AM, Bady MF, Saleh NM (2014) Environmental impact assessment of abundant lead landfill on groundwater and soil quality. *Int Water Technol J* 4:2
- El Araby M, El Arabi N (2008) Modeling potential environmental impact of new settlements on groundwater. *GéoEdmonton, Nile Delta*
- El Sayed MH, El Aassar AM, Abo El Fadl MM, Abd El Gawad AM (2012) Hydro-geochemistry and pollution problems in 10th of Ramadan city, East El Delta, Egypt. *J Appl Sci Res* 8(4):1959–1972
- El-Haddad IM (2002) Hydrogeological studies and their environmental impact on future management and sustainable development of the new communities and their surroundings, east of the Nile Delta, Egypt. Ph.D. Thesis, Faculty of Science, Mansoura University, p 435
- Elnemr A, Gad MI, Hussein EE (2015) Numerical simulation of groundwater flow and contaminant transport in the Quaternary aquifer in 10th of Ramadan city area, East Delta, Egypt. In: 8th international engineering conference. Faculty of Engineering, Mansoura University, Mansoura-Sharm El-Shikh, 17–22 Nov 2015, pp 202–222
- Embaby AE (2009) Heavy metals accumulation in soil and plants irrigated with wastewater of the 10th of Ramadan city, Geology Department, Faculty of Science at Damietta, Mansoura University, Egypt, p 21
- Embaby AA, El Haddad IM (2007) Environmental impact of wastewater on soil and groundwater at the Tenth of Ramadan City area, Egypt. *Mansoura J Geol Geophys* 34(2):25–56
- EPA (1996) Standard method 1669, sampling ambient water for trace metals at EPA water quality criteria levels
- FAO (1997) Food and Agriculture Organization: annual report on food quality control 1:11–13 and water, 5th edn, vol 1, pp 20–21
- Gad M1 (1995) Hydrogeological studies for groundwater reservoirs, east of the Tenth of Ramadan City and vicinities, M. Sc. Thesis, Ain Shams University, p 187
- Gad M, El-Kammar MM, Ismail HMG (2015) Vulnerability assessment of the Quaternary aquifer of Wadi El-Tumilat, East Delta, using different overlay and index methods. *Asian Rev Environ Earth Sci* 2(1):9–22
- Ismail HMG (2008) Study the vulnerability of groundwater aquifer for pollution in Wadi El-Tumilat, Eastern Delta. M.Sc. Thesis, Faculty of Science, Cairo University. p 286
- Khan FA, Ansari AA (2005) Eutrophication: an ecological vision. *Bot Rev* 71:449–482
- Knapp BJ, Hardy DA (2002) Nitrogen and phosphorus: Grolier educational. ISBN-10:0717275833, ISBN-13:978-0717275830
- Mondal NC, Saxena VK, Singh VS (2005) Assessment of groundwater pollution due to tannery industries in and around Dindigul, Tamilnadu, India. *Environ Geol* 48:149–157
- Nariman HK, Al Said MS, Ahmed AA (2011) Ground water in certain sites in Egypt and its treatments using a new modified ion exchange resin. *J Environ Prot* 2:435–444
- Richman M (1997) Industrial water pollution. *Wastewater* 5(2):24–29
- Saghravani SR, Mustapha S (2011) Prediction of contamination migration in an unconfined aquifer with visual MODFLOW: a case study. *World Appl Sci J* 14(7):1102–1106
- Shata AAA (1978) Genesis, formation and classification of the soils south Ismaelya canal between Belbeis and Ismaelya including Wadi El-Tumilat. M. Sc. Thesis, Faculty of Agriculture, Zagazig University, pp 1–60
- Taha AA, El Mahmoudi AS, El Haddad IM (2004) Pollution sources and related environmental impacts in the new communities South-east Nile Delta, Egypt. *Emirates J Eng Res* 9(1):35–49
- Tawfic AM, Dewedar A Mekki, Diab A (1999) The efficacy of an oxidation pond in mineralizing some industrial waste products with special reference to fluorene degradation: a case study, waste management 19 faculty of agriculture. Sues Canal University, Ismailia, pp 535–540
- Tirkey P, Bhattacharya T, Chakraborty S, Baraik S (2017) Assessment of groundwater quality and associated health risks: A CASE STUDY OF Ranchi city. India Groundwater for Sustainable Development, Jharkhand
- Umeh CN, Okorie OI, Emesiani GA (2005) Towards the provision of safe drinking water: The bacteriological quality and safety of sachet water in Awka, Anambra State. In: The book of abstract of the 29th annual conference and general meeting on microbes as agents of sustainable development. Nigerian Society for Microbiology (NSM), University of Agriculture, Abeokuta, p 22
- Waseem A, Arshad J, Iqbal F, Sajjad A, Mehmood Z, Murtaza G (2014) Pollution status of pakistan: a retrospective review on heavy metal contamination of water, soil, and vegetables. *Bio Med Research International*, vol 2014. Hindawi Publishing Corporation, Cairo, p 29
- World Health Organization standards for drinking water (WHO) (1996) International standards for drinking water, vol 1, 3rd edn. Geneva, Switzerland
- WHO (2011) Guidelines for drinking-water-quality, 4th edn. World Health Organisation, Geneva, p 541
- Wu J, Sun Z (2016) Evaluation of shallow groundwater contamination and associated human health risk in an Alluvial Plain impacted by agricultural and industrial activities, Mid-west China. *Expo Health* 8:311–329
- Zheng C (2006) MT3DMS: A modular three-dimensional multispecies transport model for simulation of advection, dispersion and chemical reactions of contaminants in groundwater systems. Department of Geological Sciences, University of Alabama, p 46. <http://hydro.geo.ua.edu/mt3d/>

Publisher's Note Springer Nature remains neutral with regard to jurisdictional claims in published maps and institutional affiliations.